



QED Effects in Parton Evolution

Work Project within the DESY Summer Student Programme

Florian Fabry
WWU Münster, Germany

September 22, 2019

Supervisor: Markus DIEHL, DESY Theory Group

Contents

1. PDFs and the DGLAP equation	2
1.1. Introduction	2
1.2. Discretizing the DGLAP equation in the Chebychev basis	5
2. Solving the coupled RGEs of QCD and QED up to NNLO	7
2.1. Original version	7
2.2. Expressing α_e in terms of α_s	9
3. The evolution basis	15
4. Implementation of QED and $\text{QED} \otimes \text{QCD}$ splitting kernels	19
5. Numerical Results	23
A. Explicit shape of coupled RGE solutions	26
B. Full NLO color-stripped evolution equations	29

Acknowledgments

My sincere thanks go to my supervisor Markus Diehl, for offering me the opportunity to have worked on such an exciting topic and constantly providing support and assistance on the way. In addition, I would like to thank Riccardo Nagar for many enlightening discussion about PDFs in general and a very instructive introduction to `chilipdf` in particular. Especially on the topic of coupled RGEs, Georgios Billis and Frank Tackman were a great help. I am thankful for the numerous discussions and advices. At last, I want to show gratitude to the DESY and the organization team of the Summer School Programme for giving many students the chance to widen their knowledge and gain new experiences.

1. PDFs and the DGLAP equation

1.1. Introduction

Hadrons, especially protons and neutrons, make up a huge proportion of visible matter and, in addition, are one of the most commonly examined objects in experimental and theoretical particle physics. Formed by quarks and bound together by gluons, hadrons are one of the best examples when studying the effects of QCD. However, since QCD is asymptotically free, bound states like hadrons cannot be analyzed perturbatively. Hence, when describing hadronic structures, one needs the help of non-perturbative objects, the so-called parton distributions functions (PDFs). These densities f describe the probability of finding a parton of the hadron, which classically are quarks and the gluon, at a certain momentum fraction¹ x . A detailed introduction can be found in every dedicated textbook, e.g. [Peskin and Schroeder, 1995], chapter 14, and parts of chapter 17 and 18.

Consider now a process involving at least one hadron. If hadrons are non-perturbative objects, it is not obvious that one can calculate the actual process, e.g. an electron scattering off the hadron, perturbatively. That this is actually possible, is proven by the famous Factorization theorem. The word "factorization" can be taken literal, as by using this statement one is able to separate the actual process from all hadronic subprocesses.

One could even go one step further: There is a way to identify and calculate the perturbative part of the hadronic structure, meaning the PDFs itself. Factorization introduces a so-called factorization scale μ , which, as an artificial parameter, the physical cross section must be independent of. Analogous to renormalization group equations (RGEs), one can use this fact to introduce an equation to describe the scaling of the PDFs, the DGLAP (Dokshitzer-Gribov-Lipatov-Altarelli-Parisi) equation. What is left as the non-perturbative part is the x -dependence of the PDF at some starting scale μ_0 . To obtain this (analytic) expression, one needs to fit a parameter function to experimental data.

For any desired PDF, the DGLAP equation has the form

$$\frac{df(x, \mu)}{d \ln \mu} = P(x, \mu) \otimes f(x, \mu) \quad (1.1)$$

The equation above introduces the so-called splitting kernels $P(x, \mu)$, which encode

¹ To be more precise: The Bjorken x actually is a kinematic variable, $x = -\frac{q^2}{2P \cdot q}$, where P and q are the four-momenta of Proton and the momentum transfer in some arbitrary process. In the parton model, this variable can be identified with the momentum fraction, historically denoted by ξ .

1. PDFs and the DGLAP equation

the relation between different PDF flavors. In general, the right-hand-side contains a sum over all flavors, giving rise to many different kernels, but we will drop this sum for reasons of simplicity in this chapter². These kernels are perturbative objects, which makes the DGLAP equation at least numerically solvable.

Due to the huge coupling strength of QCD α_s , compared to e.g. α_e , the dominating diagrams for the kernels of quarks and gluons are QCD-diagrams. Figure 1.1a shows an exemplary diagram contributing to P_{qq} . The objective of this work will be to extend these graphs by QED contributions. These contributions include pure QED graphs, see figures 1.1b, and mixed ones like figure 1.1c. Further details on efficiently handling these graphs in every specific case can be found in chapter 4. To keep things consistent, one needs to add new PDFs, i.e. new constituents of the hadron, when also taking QED into account. Namely, these contributions are the fields of the QED-Lagrangian: Leptons and the photon. These new PDFs of course also alter the existing pure QCD sector by new splitting functions, e.g. $P_{g\gamma}$.

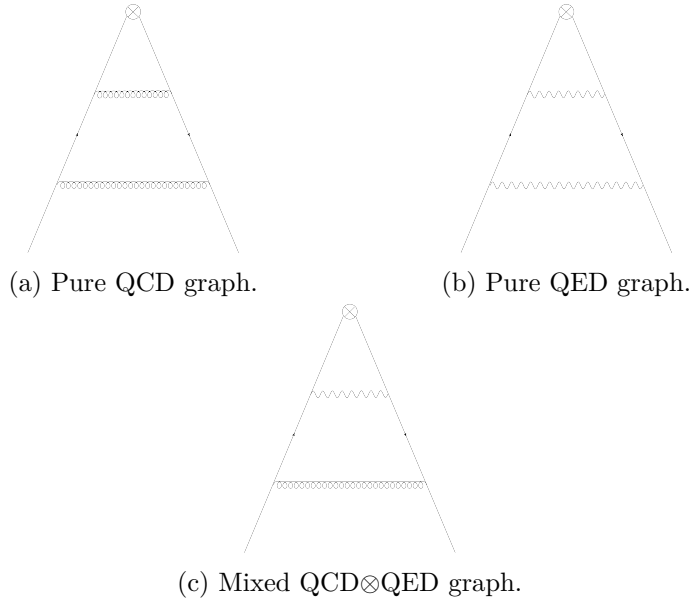


Figure 1.1.: Examples for splitting functions with different interactions. The cross at the upper ends of the graphs symbolizes the hard scattering, perturbative part. There is an implicit cut through the middle of the diagram representing a squared amplitude and putting all intermediate particles on-shell.

After setting up all new and altered evolution equations, they will be implemented in `chilipdf`, a PDF interpolator and evolver being currently in development. To numerically solve the DGLAP equation, `chilipdf` uses a numerically very precise

² Alternatively, one can think of (1.1) as an equation for a vector of PDFs, turning P into a matrix of kernels.

1. PDFs and the DGLAP equation

approximation with Chebychev polynomials, being explained in the next chapter.

1.2. Discretizing the DGLAP equation in the Chebychev basis

For now, let us turn back to the DGLAP equation, see (1.1). By expanding the PDFs in the basis of Chebychev-polynomials one can separate the x - and μ -dependence:

$$f(x, \mu) = \sum_{k=0}^{\infty} f_k(\mu) T_k(x). \quad (1.2)$$

In addition, by substituting (1.2) into (1.1) the DGLAP equation reduces to a differential equation for every $f_k(\mu)$ ³:

$$\frac{df_k}{d \ln \mu} = \sum_{k'=0}^{\infty} P_{kk'}(\mu) f_{k'}(\mu), \quad (1.3)$$

where

$$P_{kk'}(\mu) = \quad (1.4)$$

Perturbation theory implies that one can expand the splitting functions into a series in α_s :

$$P(x, \mu) = \alpha_s(\mu) P^{10}(x) + \alpha_e(\mu) P^{01}(x) + \alpha_s^2(\mu) P^{20}(x) + \alpha_s \alpha_e P^{11}(x) + \alpha_e^2(\mu) P^{02}(x) + \mathcal{O}(\alpha_{s,e}^3). \quad (1.5)$$

A similar expansion is of course also valid for the $P_{kk'}(x)$ coefficients.

There are two major points against numerically solving (1.3) via a well-known Runge-Kutta algorithm. Since μ is an energy scale, the stepwidth needs to be rather small compared to other scales if one wants to cover a wide range of values. Additionally, $P(x, \mu)$ only depends on μ via $\alpha_s(\mu)$ and $\alpha_e(\mu)$. Therefore, changing variables to a strong coupling would cause tremendous numerical advantages. The reason being is that variable The coupling dependence of the leading term in (1.5) completely or nearly cancels. This makes the kernel constant in first approximation, which greatly improves the numerical accuracy of the Runge-Kutta algorithm. Our choice will be α_s^{QCD} , carrying just the QCD dependence in its β function. The scale dependence of $\alpha_s^{\text{QCD}}(\mu)$ is determined by the Renormalization Group Equation (2.12), which implies⁴

$$\frac{df_k(\alpha_s^{\text{QCD}})}{d\alpha_s^{\text{QCD}}} = \frac{1}{\alpha_s^{\text{QCD}} \beta_s(\alpha_s^{\text{QCD}}, 0)} \sum_{k'=0}^{\infty} P_{kk'}(\alpha_s(\alpha_s^{\text{QCD}}), \alpha_e(\alpha_s^{\text{QCD}})) f_{k'}(\alpha_s^{\text{QCD}}). \quad (1.6)$$

The original $f_k(\mu)$ can then later be reobtained by substituting the solution of the RGE, i.e. $f_k(\mu) = f_k(\alpha_s^{\text{QCD}}(\mu))$. Note that with this choice the leading term in ever

³ This means nothing less than discretising the integral of the Mellin convolution.

⁴ For further details on α_s^{QCD} see chapter 2.

1. PDFs and the DGLAP equation

$P_{kk'}$ is nearly constant, since QED corrections are small. If one would just expand up to $\mathcal{O}(\alpha_s^1, \alpha_e^0)$, the right-hand-side is yet completely constant.

The equation above contains two subtleties, which makes this approach harder than it seems at first sight. First, we are forced to compute the running of α_e in terms of α_s . This can only be achieved by reformulating the coupled system of RGEs for α_s and α_e , which is the objective of the next chapter. In addition, the splitting kernel now also contains pure QED and coupled QCD \otimes QED effects, which will be discussed later.

2. Solving the coupled RGEs of QCD and QED up to NNLO

2.1. Original version

In this chapter we will discuss the so-called iterative solutions. What motivates an approximate analytical solution compared to a numerical, e.g. Runge-Kutta, one, which is precise up to machine precision, is the fast evaluation of the closed analytical form.

Before looking at $\alpha_e(\alpha_s)$ the first step will be to solve the original system of RGEs. We start with the coupled Renormalization Group Equations (RGE) for QCD and QED at NNLO:

$$\begin{aligned} \frac{d\alpha_s}{d\ln\mu} &= \beta_s(\alpha_s(\mu), \alpha_e(\mu)) \\ &= -\frac{\beta_{00}^s}{2\pi} \alpha_s^2(\mu) \left(1 + \epsilon_s b_{10}^s \alpha_s(\mu) + \epsilon_e b_{01}^s \alpha_e(\mu) \right. \\ &\quad \left. + b_{20}^s \alpha_s^2(\mu) + b_{11}^s \alpha_s(\mu) \alpha_e(\mu) + b_{02}^s \alpha_e^2(\mu) + \mathcal{O}(\epsilon_{s,e}^3) \right) \end{aligned} \quad (2.1)$$

$$\begin{aligned} \frac{d\alpha_e}{d\ln\mu} &= \beta_e(\alpha_e(\mu), \alpha_s(\mu)) = \\ &= \frac{\beta_{00}^e}{2\pi} \alpha_e^2(\mu) \left(1 + \epsilon_e b_{10}^e \alpha_e(\mu) + \epsilon_s b_{01}^e \alpha_s(\mu) \right. \\ &\quad \left. + b_{20}^e \alpha_e^2(\mu) + b_{11}^e \alpha_e(\mu) \alpha_s(\mu) + b_{02}^e \alpha_s^2(\mu) + \mathcal{O}(\epsilon_{e,s}^3) \right) \end{aligned} \quad (2.2)$$

We have introduced artificial expansion parameters $\epsilon_{s,e}$ for both couplings to keep track of the order we want to expand to. Following [Billis et al., 2019], we have defined

$$b_{mn}^{s,e} \equiv \frac{1}{(4\pi)^{m+n}} \cdot \frac{\beta_{mn}^{s,e}}{\beta_{00}^{s,e}} \quad (2.3)$$

Note that there is no asymptotic freedom in QED, hence there are no overall minus signs in the $\beta_{m,n}^e$ constants. The coefficients of $\beta_{e,s}$ can be explicitly calculated by renormalizing $\alpha_{s,e}$ at the according order of the expansion.

In this report we will apply the method of iterative solutions, fully explained in [Billis et al., 2019]. In this paper, one also can find iterative solutions of the RGE system above up to NNLO, which we will discuss in the following.

Solving these equations up to leading order (i.e. just keeping the leading term in

2. Solving the coupled RGEs of QCD and QED up to NNLO

both expansions) gives after a trivial integration:

$$\alpha_s^{\text{LO}}(\mu) = \frac{\alpha_s(\mu_0)}{X_s(\mu, \mu_0)} \quad (2.4)$$

$$\alpha_e^{\text{LO}}(\mu) = \frac{\alpha_e(\mu_0)}{X_e(\mu, \mu_0)}, \quad (2.5)$$

where

$$X_{s,e}(\mu, \mu_0) \equiv 1 + \frac{\alpha_{s,e}(\mu_0)}{2\pi} \beta_{00}^{s,e} \ln\left(\frac{\mu}{\mu_0}\right). \quad (2.6)$$

The boundary conditions are given by

$$\mu_0 = m_Z, \quad (2.7)$$

$$\alpha_s(\mu_0) = 0.118 \quad (2.8)$$

$$\text{and } \alpha_e(\mu_0) = \frac{1}{127}. \quad (2.9)$$

To compute the NLO solution (i.e. the solution of order 1), we discuss the approach for the iterative solution of an arbitrary order n : First expand the RGEs to the appropriate order, which we have already done in equations (2.1) and (2.2) for the NLO solution. Then substitute the in ϵ_s and ϵ_e expanded iterative solutions of order $n-1$ in all terms, while keeping the overall factor $\alpha_{s,e}^2(\mu)$ in front of the expansion exact. This implies that in order to obtain the n -th order solution, one already must have calculated all solutions of lower order.

For the NLO case ($n=1$) we are exactly in this situation. At first tackling $\alpha_s(\mu)$ by substituting the LO solutions (2.4) and (2.5) into (2.1) (truncated by the terms of order 2), we arrive at

$$\alpha_s^{\text{NLO}}(\mu) = \alpha_s(\mu_0) \left[X_s(\mu, \mu_0) + \frac{\alpha_s(\mu_0)}{2\pi} \left(\epsilon_s b_{10}^s \ln(X_s(\mu, \mu_0)) + \epsilon_e b_{01}^s b_{01}^s \ln(X_e(\mu, \mu_0)) \right) \right]^{-1} \quad (2.10)$$

after separation of variables, changing the integration variable from $\ln \mu$ to $X_s(\mu, \mu_0)$ or $X_e(\mu, \mu_0)$ on the right-hand-side and performing the now again trivial integration. $\alpha_e^{\text{NLO}}(\mu)$ can then be obtained by just interchanging $s \leftrightarrow e$ in the equation above.

Solving the full NNLO equations (2.1) and (2.2), which introduces slightly more difficult integrals, follows exactly the same steps. We arrive at

$$\begin{aligned} \frac{\alpha_s(\mu_0)}{\alpha_s(\mu)} = & X_a + \epsilon_a \frac{\alpha_a(\mu_0)}{4\pi} b_{10}^a \ln X_a + \epsilon_a^2 \frac{\alpha_a(\mu_0)^2}{(4\pi)^2} \left(b_{20}^a \frac{X_a - 1}{X_a} + (b_{10}^a)^2 \frac{1 - X_a + \ln X_a}{X_a} \right) \\ & + \epsilon_b \frac{\alpha_a(\mu_0)}{4\pi} b_0^a b_{01}^a \ln X_b + \epsilon_b^2 \frac{\alpha_a(\mu_0) \alpha_b(\mu_0)}{(4\pi)^2} b_0^a \left(b_{02}^a \frac{X_b - 1}{X_b} + b_{01}^a b_{10}^b \frac{1 - X_b + \ln X_b}{X_b} \right) \\ & + \epsilon_a \epsilon_b \frac{\alpha_a(\mu_0)}{b_0^a \alpha_a(\mu_0) - \alpha_b(\mu_0)} \left[\frac{\alpha_a^2(\mu_0)}{(4\pi)^2} (b_0^a)^2 b_{10}^a b_{01}^a \left(\frac{X_b}{X_a} \ln X_b - \frac{1 - X_b}{1 - X_a} \ln X_a \right) \right. \\ & \left. - \frac{\alpha_b^2(\mu_0)}{(4\pi)^2} b_{01}^a b_{01}^b \left(\frac{X_a}{X_b} \ln X_a - \frac{1 - X_a}{1 - X_b} \ln X_b \right) + \frac{\alpha_a(\mu_0) \alpha_b(\mu_0)}{(4\pi)^2} b_0^a b_{11}^a \ln \frac{X_a}{X_b} \right], \end{aligned} \quad (2.11)$$

2. Solving the coupled RGEs of QCD and QED up to NNLO

where again one just needs to interchange $s \leftrightarrow e$ to obtain $\alpha_e^{\text{NNLO}}(\mu)$.

On page 9 of [Billis et al., 2019] one can find detailed plots concerning the accuracy of all solutions up to NNLO by using the relative error, which will be defined in the next chapter.

2.2. Expressing α_e in terms of α_s

Having now the NLO solution of the original system at hand, let us change variables in the RGE of QED. At first sight, the natural choice for the new running variable would be the full QCD coupling. Nevertheless, it is actually more convenient to use just the part of α_s which obeys the pure QCD β -function:

$$\frac{d\alpha_s^{\text{QCD}}}{d\ln\mu} = \beta_s(\alpha_s^{\text{QCD}}, 0). \quad (2.12)$$

If we would now change α_s^{QCD} , we would run into some nontrivial problems when trying to obtain the NLO solution of $\alpha_s - \alpha_s^{\text{QCD}}$. Hence, to get rid of the overall α^2 factor in every RGE, we first introduce new variables

$$r_e \equiv \frac{\alpha_e(\mu_0)}{\alpha_e} - 1 \quad (2.13)$$

$$\text{and } r_s \equiv \frac{\alpha_s^{\text{QCD}}(\mu_0)}{\alpha_s^{\text{QCD}}} - 1. \quad (2.14)$$

We also added a shift and a factor to obtain as simple boundary conditions as possible, see (2.22). This gives

$$\frac{dr_s}{d\ln\mu} = \alpha_s(\mu_0)\beta_s\left(\frac{\alpha_s(\mu_0)}{r_s + 1}, 0\right) \equiv \tilde{\beta}_s(r_s, 0). \quad (2.15)$$

for the pure QCD RGE. We define a difference to the full QCD coupling,

$$\delta_r = r_s^{\text{full}} - r_s, \quad (2.16)$$

to recover expressions for the original couplings:

$$\alpha_e(r_s, r_e) = \frac{\alpha_e^0}{r_e(r_s) + 1} \quad (2.17)$$

$$\alpha_s(r_s, \delta_r) = \frac{\alpha_s^0}{r_s + \delta_r(r_s) + 1} \quad (2.18)$$

Changing variables in the remaining two equations yields

$$\frac{dr_e}{dr_s} = \frac{\tilde{\beta}_e(r_e, r_s + \delta_r)}{\tilde{\beta}_s(r_s, 0)} \quad (2.19)$$

$$\frac{d\delta_r}{dr_s} = \frac{\tilde{\beta}_s(r_s + \delta_r, r_e)}{\tilde{\beta}_s(r_s, 0)} - 1 \quad (2.20)$$

2. Solving the coupled RGEs of QCD and QED up to NNLO

Additionally, it is the simplest to change from $\ln \mu$ to

$$t \equiv \ln \frac{\mu}{\mu_0}. \quad (2.21)$$

With these definitions the new boundary conditions read

$$r_s(0) = \delta_r(0) = r_e(0) = 0. \quad (2.22)$$

The differential equations above remain the same since $dt = d \ln \mu$.

We will now give the iterative solution up to NNLO (computed in exactly the same way as the ones in chapter 2.1), beginning with r_s . One can show just by resubstituting that the following results are equivalent to the ones given in chapter 2.1.

$$\begin{aligned} r_s^{\text{NNLO}}(t) = & \beta_{00}^s \alpha_s^0 t + \epsilon_s b_{10}^s \alpha_s^0 \ln(1 + \beta_{00}^s \alpha_s^0 t) \\ & + \epsilon_s^2 (\alpha_s^0)^2 \frac{(b_{10}^s)^2 \left(\ln(1 + \beta_{00}^s \alpha_s^0 t) - \beta_{00}^s \alpha_s^0 t \right) + b_{20}^s \beta_{00}^s \alpha_s^0 t}{1 + \beta_{00}^s \alpha_s^0 t} \end{aligned} \quad (2.23)$$

For the sake of clarity, from now on we use the abbreviation $\alpha_{s,e}(\mu_0) \equiv \alpha_{s,e}^0$.

The LO solutions for (2.19) and (2.20) are rather simple:

$$r_e^{\text{LO}}(r_s) = \alpha^0 t \quad (2.24)$$

$$\delta_r^{\text{LO}}(r_s) = 0, \quad (2.25)$$

where we have used

$$\alpha^0 \equiv \frac{\beta_{00}^e \alpha_e^0}{\beta_{00}^s \alpha_s^0}. \quad (2.26)$$

Let us now solve (2.19) at NLO. If we substitute the LO solutions above the equation reads (after some rewriting)

$$\begin{aligned} \frac{dr_e}{dr_s} = & \alpha^0 \frac{\alpha^0 r_s^2 + (1 + \alpha^0 + \epsilon_e b_{10}^e \alpha_e^0 + \epsilon_s b_{01}^e b_0^e \alpha_e^0) r_s + 1 + \epsilon_e b_{10}^e - 0 + \epsilon_s b_{01}^e \alpha_s^0}{\alpha^0 r_s^2 + (1 + \alpha^0 + \epsilon_s b_{10}^s b_0^e \alpha_e^0) r_s + 1 + \epsilon_s b_{10}^s \alpha_s^0} \\ \equiv & \alpha^0 f_e^{\text{NLO}}(r_s). \end{aligned} \quad (2.27)$$

Integrating gives

$$r_e(r_s) = \alpha^0 (F_e^{\text{NLO}}(r_s) - F_e^{\text{NLO}}(0)), \quad (2.28)$$

where we defined F_e^{NLO} fulfills $\frac{d}{dr_s} F_e^{\text{NLO}}(r_s) = f_e^{\text{NLO}}(r_s)$. The explicit expression of $F_e^{\text{NLO}}(\alpha_s)$ is given in the appendix A.

In exactly the same way, one is able to find the NLO solution for $\delta_r(r_s)$. The equation

$$\begin{aligned} \frac{d\delta_r}{dr_s} = & \frac{\alpha^0 r_s^2 + (1 + \alpha^0 + \epsilon_s b_{10}^s b_0^e \alpha_e^0 + \epsilon_e b_{01}^s b_0^e \alpha_e^0) r_s + 1 + \epsilon_s b_{10}^s \alpha_s^0 + \epsilon_e b_{01}^s \alpha_e^0}{\alpha^0 r_s^2 + (1 + \alpha^0 + \epsilon_s b_{10}^s b_0^e \alpha_e^0) r_s + 1 + \epsilon_s b_{10}^s \alpha_s^0} - 1 \\ = & f_\delta^{\text{NLO}}(r_s) \end{aligned} \quad (2.29)$$

2. Solving the coupled RGEs of QCD and QED up to NNLO

implies again a result of the form

$$\delta_r^{\text{NLO}}(r_s) = F_\delta^{\text{NLO}}(r_s) - F_\delta^{\text{NLO}}(0), \quad (2.30)$$

where $F_\delta^{\text{NLO}}(r_s)$ is given in appendix A.

One way to justify these results is to compare it with the solution obtained by numerically solving the NLO system. Relative errors, defined as

$$\Delta h_{\text{rel}}(x) \equiv \frac{|h(x)^{\text{sol}}(\mu) - h(x)^{\text{num}}(\mu)|}{h(x)^{\text{num}}(\mu)} \quad (2.31)$$

for any function $h(x)$ (obeying an according differential equation) relate different iterative solutions $h(x)^{\text{sol}}(\mu)$ to the numerical solution $h(x)^{\text{num}}(\mu)$, which is exact up to machine precision. Figure 2.1 shows the relative errors of α_e , δ_r and α_s . These get compared with relative errors of iterative solutions of the original, μ dependent coupled system of $\alpha_s(\mu)$ and $\alpha_e(\mu)$, which can be obtained in exactly the same way as described above. For further details, see [Billis et al., 2019], chapter 2.2.

2. Solving the coupled RGEs of QCD and QED up to NNLO

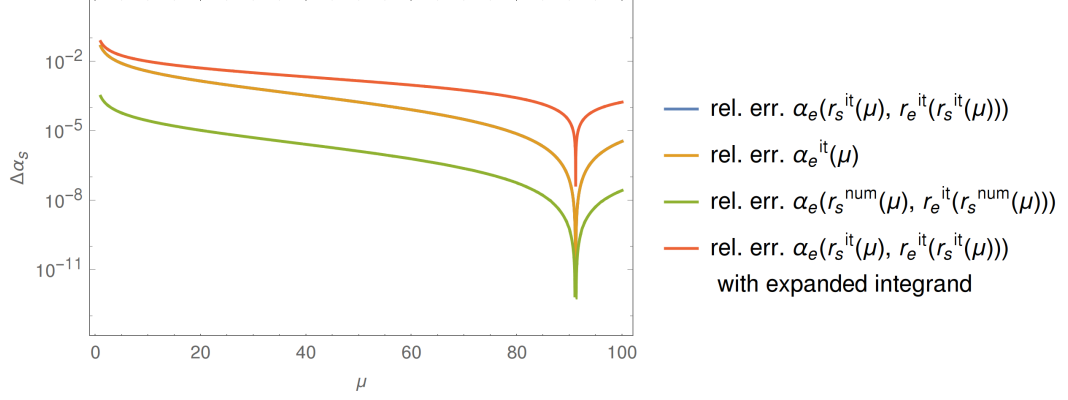


Figure 2.1.: Shown are of the relative errors in per cent of $\alpha_e(r_s(\mu), r_e^{\text{NLO}}(r_s(\mu)))$ (see (2.28)), with iterative (see (2.23) up to NLO) and numerical solutions of $r_s(\mu)$ inserted, a version of $r_e(r_s)$, where one expanded the integrand before integrating and the iterative solution of $\alpha_s(\mu)$ (see (2.11) up to NLO). μ ranges from 1 GeV to 100 GeV. The blue ($\alpha_e^{\text{it}}(\mu)$) and yellow ($\alpha_e(r_s^{\text{it}}(\mu), r_e^{\text{NLO}}(r_s^{\text{it}}(\mu)))$) line completely overlap.

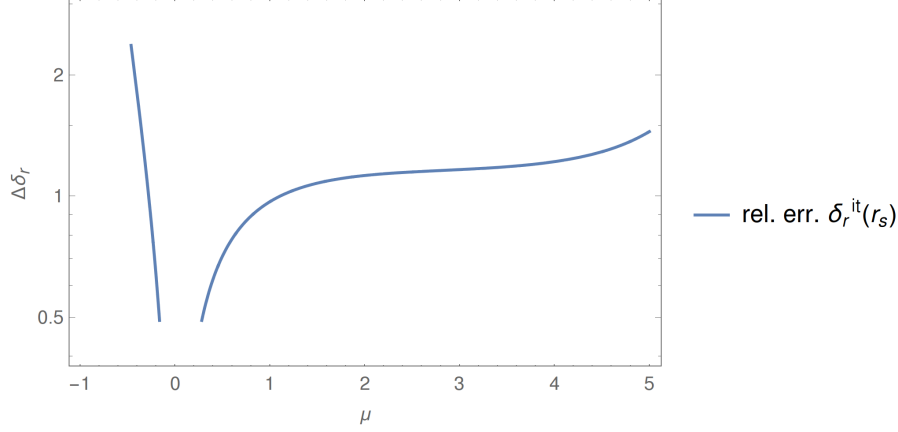


Figure 2.2.: Relative errors in per cent of δ_r^{NLO} (see (2.30)) depending on r_s , which ranges from -0.99 to 5 .

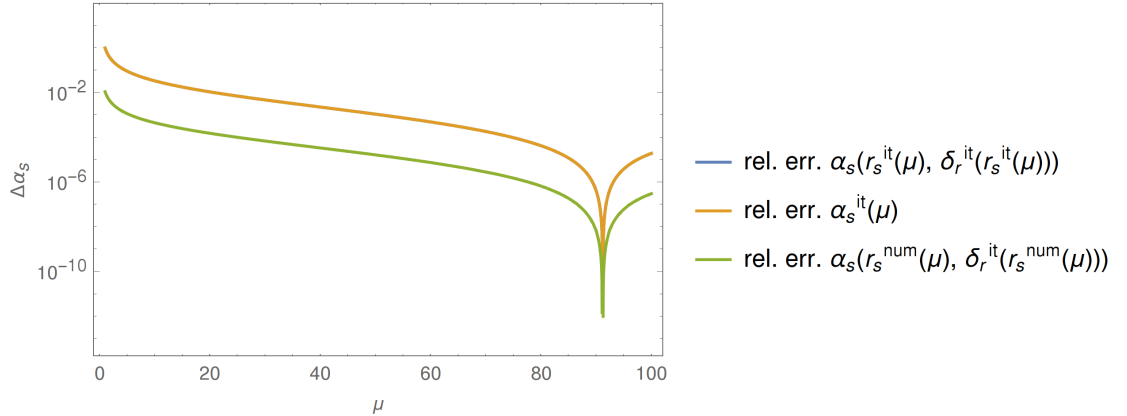


Figure 2.3.: Comparison of the relative errors in per cent of $\alpha_s(r_s(\mu), \delta_r^{\text{NLO}}(r_s(\mu)))$, with iterative (see (2.23)) and numerical solutions of $r_s(\mu)$ inserted, with the iterative solution of $\alpha_s(\mu)$ (see (2.11) up to NLO). μ ranges from 1 GeV to 100 GeV.

2. Solving the coupled RGEs of QCD and QED up to NNLO

It is impossible to distinguish between the errors of the iterative solutions obtained via the r -method and directly via $\alpha_{s,e}$, which confirms the analytical equivalence of both approaches¹. Inserting the numerical solution for r_s instead of the iterative one decreases the error by roughly two orders of magnitude, thus this option will be implemented into the final code. Exactly the same is the case for $r_s^{\text{full}} = r_s + \delta_r$.

At last, one could expand $i^{\text{NLO}}(r_s)$ up to $\mathcal{O}(\epsilon_s, \epsilon_e)$, which leaves a rather easy integration. This simplification costs about one order of magnitude in the relative error. Although not necessary here, since the integration is analytically doable, this gives an estimate for NNLO, where this is not the case anymore.

The relative error of δ_r lies in the region of 1%, but intrinsically goes with ϵ_e and therefore does not have to reach as low values as e.g. r_e .

Via a numerical solution of the inversion of (2.15) one can deduce that these corresponds to energies between approximately 0 GeV and 10^{18} GeV.

To obtain the NNLO solutions $r_e^{\text{NNLO}}(r_s)$ and $\delta_r^{\text{NNLO}}(r_s)$, we actually need to vary the established pattern. Since in this case we deal with a fraction of β functions, we substitute the complete iterative NLO solution (2.28). In general, with $r_e^{\text{NLO}}(r_s)$ and $\delta_r^{\text{NLO}}(r_s)$ containing a combination of areatangiens hyperbolicus and logarithms, the explicit integration of this expression is not possible. Hence we expand the right-hand-sides and then perform the integration, leading to a similar shape as the NLO-solution:

$$r_e^{\text{NNLO}} = \alpha^0 (F_e^{\text{NNLO}}(r_s) - F_e^{\text{NNLO}}(0)) \quad (2.32)$$

$$\delta_r^{\text{NNLO}}(r_s) = F_\delta^{\text{NNLO}}(r_s) - F_\delta^{\text{NNLO}}(0) \quad (2.33)$$

Again, $F_e^{\text{NNLO}}(r_s)$ and $F_\delta^{\text{NNLO}}(r_s)$ are given in the appendix A.

One can compare these solutions with one of the approximations of $\alpha_e^{\text{NNLO}}(\alpha_s)$ in figure 2.1, which yields a deviation by an approximate factor of 10 with respect to the complete iterative solution. Figure 2.4 shows the relative errors of α_e , δ_r and α_s at NNLO.

Due to the additional expansion of the integrand, we see that the error of the iterative solution of $r_e(r_s)$ increases compared to the one of $\alpha_e(\mu)$. Inserting the numerical solution of $r_e(\mu)$ does not lead to such a high improvement as in the case of NLO. The relative error of δ_r diverges at $r_s = 0$, which can be traced back to a root of $\delta_r(r_s)$ at this value. Apart from that, the error is comparatively high but still in an acceptable region due to the smallness of $\delta_r \propto \epsilon_e$.

To conclude, even after applying the necessary expansion of the integrand, the relative error of the iterative solution for $\alpha_e(\alpha_s^{\text{QCD}})$ does not exceed 0.1% and therefore is suitable for an implementation in the `chilipdf` code.

¹ After some algebra, this equivalence can also be seen directly in the equations.

2. Solving the coupled RGEs of QCD and QED up to NNLO

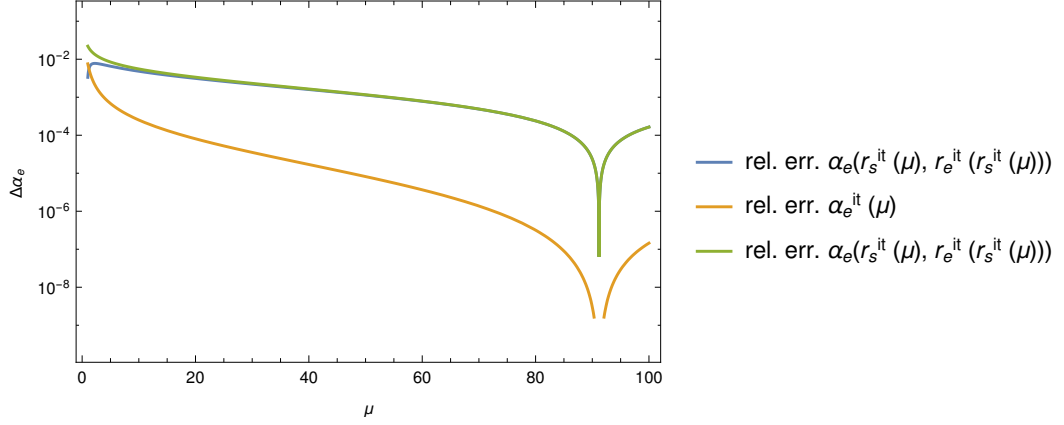


Figure 2.4.: Shown are of the relative errors in per cent of $\alpha_e(r_s(\mu), r_e^{\text{NNLO}}(r_s(\mu)))$ (see (2.32)), with iterative (see (2.23) up to NNLO) and numerical solutions of $r_s(\mu)$ inserted, a version of $r_e(r_s)$, where one expanded the integrand before integrating and the iterative solution of $\alpha_s(\mu)$ (see (2.11) up to NNLO). μ ranges from 1 GeV to 100 GeV.

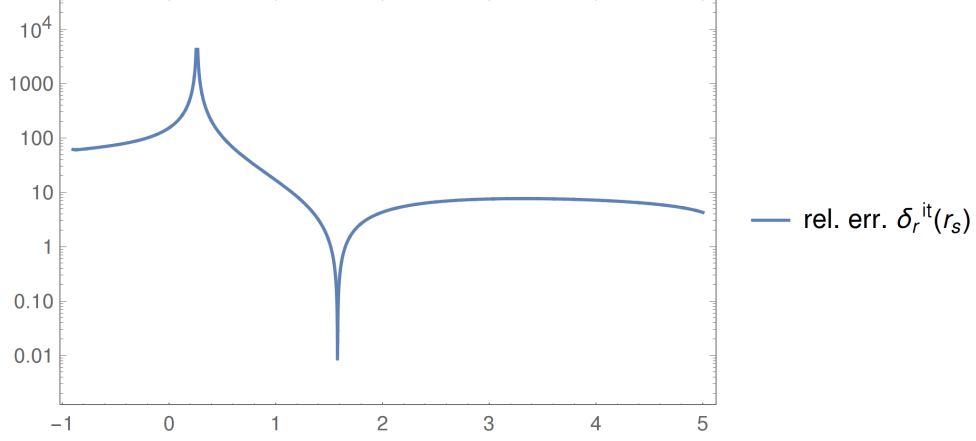


Figure 2.5.: Relative error of $\delta_r^{\text{NNLO}}(r_s)$ (see (2.33)) with r_s ranges from -0.99 to 5 .

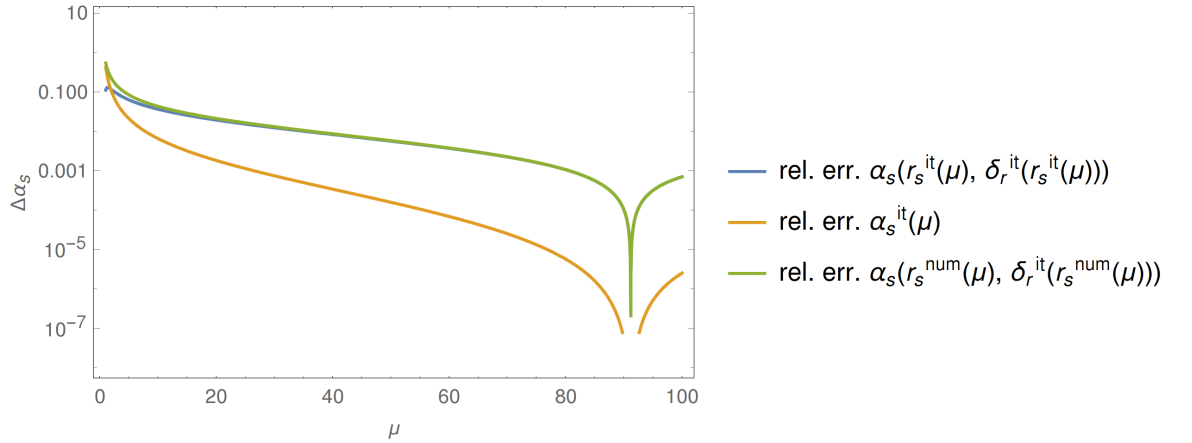


Figure 2.6.: Comparison of the relative errors of $\alpha_s(r_s(\mu), \delta_r^{\text{NNLO}}(r_s(\mu)))$ (see (2.23)), with iterative (see (2.23)) and numerical solutions of $r_s(\mu)$ inserted, with the iterative solution of $\alpha_s(\mu)$ (see (2.11)). μ ranges from 1 GeV to 100 GeV.

3. The evolution basis

The development of including QED interactions in splitting kernels can be comprehended in the publications [Roth and Weinzierl, 2004] ($\mathcal{O}(\alpha_e)$, photon PDF), [Bertone et al., 2015] ($\mathcal{O}(\alpha_e)$, lepton PDFs), [de Florian et al., 2017b] ($\mathcal{O}(\alpha_e^2)$) and [de Florian et al., 2017a] ($\mathcal{O}(\alpha_e\alpha_s)$).

Before discussing the QED extensions of the splitting kernels, one needs to work out the interplay between all active PDFs in the hadron via different kernels. Besides the classical "QCD" PDFs, the gluon g and active quarks, this also includes the photon γ and all active leptons l_i . Since up and down quarks have distinct (QED-) charges, we will distinguish between their PDFs using an u_i and d_i . In the definitions above, i runs up to the according (active) flavor number n_u , n_d and n_l .

In this physical, so-called parton basis, the evolutions equations look as follows¹:

$$\frac{dg}{dt} = P_{gg}g + P_{g\gamma}\gamma + \sum_f (P_{gf}f + P_{g\bar{f}}\bar{f}) \quad (3.1)$$

$$\frac{d\gamma}{dt} = P_{\gamma\gamma}g + P_{\gamma g}\gamma + \sum_f (P_{\gamma f}f + P_{\gamma\bar{f}}\bar{f}) \quad (3.2)$$

$$\frac{du_i}{dt} = P_{qg}g + P_{u\gamma}\gamma + \sum_f (P_{uf}f + P_{u\bar{f}}\bar{f}) \quad (3.3)$$

$$\frac{dd_i}{dt} = P_{qg}g + P_{d\gamma}\gamma + \sum_f (P_{df}f + P_{d\bar{f}}\bar{f}) \quad (3.4)$$

$$\frac{dl_i}{dt} = P_{lg}g + P_{l\gamma}\gamma + \sum_f (P_{lf}f + P_{l\bar{f}}\bar{f}) \quad (3.5)$$

$$\frac{d\bar{u}_i}{dt} = P_{\bar{q}g}g + P_{\bar{u}\gamma}\gamma + \sum_f (P_{\bar{u}f}f + P_{\bar{u}\bar{f}}\bar{f}) \quad (3.6)$$

$$\frac{d\bar{d}_i}{dt} = P_{\bar{q}g}g + P_{\bar{d}\gamma}\gamma + \sum_f (P_{\bar{d}f}f + P_{\bar{d}\bar{f}}\bar{f}) \quad (3.7)$$

$$\frac{d\bar{l}_i}{dt} = P_{\bar{l}g}g + P_{\bar{l}\gamma}\gamma + \sum_f (P_{\bar{l}f}f + P_{\bar{l}\bar{f}}\bar{f}) \quad (3.8)$$

In the equations above, we already used some simplifications: There is no difference between different quarks when interacting with a gluon, thus just one P_{qg} and

¹ For the sake of clarity, we write the Mellin-convolution " \otimes " as a simple product. Hence, by following the formalism established in chapter 1, we treat the kernels as matrices and PDFs as vectors.

3. The evolution basis

P_{gq} is sufficient to describe this mixing, respectively. In addition, up- and down-quarks have good quantum number also when taking QED interactions into account, meaning that we do not have to introduce splitting kernels for each individual quark, but just for up- and down-flavors in general. This will also greatly simplify the sums over all fermions f . Furthermore, this motivates a change of basis to make as many of the equations above diagonal as possible. To motivate the so-called evolution basis, we first note that kernels involving one fermion f and one gauge boson b do not change when the fermion into an antifermion:

$$P_{fb} = P_{\bar{f}b}. \quad (3.9)$$

Furthermore, charge invariance of all kernels yields

$$P_{f\bar{f}} = P_{\bar{f}f} \text{ and } P_{ff} = P_{\bar{f}\bar{f}}. \quad (3.10)$$

This implies, that the so-called valence distribution

$$f^- \equiv f - \bar{f} \quad (3.11)$$

of an arbitrary fermion decouples from both the gluon and the photon:

$$\frac{df^-}{dt} = P_f^- f^- + \sum_{f'} \Delta P_{ff'}^S f'^-, \quad (3.12)$$

where we have used some of the following common kernel definitions:

$$P_{fif_j} \equiv \delta_{ij} P_{ff}^V + P_{fif_j}^S \quad (3.13)$$

$$P_{fi\bar{f}_j} \equiv \delta_{ij} P_{f\bar{f}}^V + P_{fi\bar{f}_j}^S \quad (3.14)$$

$$P_f^\pm \equiv P_{ff}^V \pm P_{f\bar{f}}^V \quad (3.15)$$

$$\Delta P_{ff'} \equiv P_{ff'} - P_{f\bar{f}'} \quad (3.16)$$

$$\bar{P}_{ff'} \equiv P_{ff'} + P_{f\bar{f}'} \quad (3.17)$$

for arbitrary fermions f_i, f_j, f and f'^2 . We can get rid of the sum over all fermions f in (3.12) by taking the difference between two flavors with the same quantum numbers, namely between two up-quarks, down-quarks or leptons. To keep these differences as small as possible, which minimizes the numerical uncertainties of these distributions, we take differences of consecutive flavors ordered by their mass. In the case of all flavors active, $n_u = n_d = n_l = 3$, we have the basis elements³

$$q_{uc}^- \equiv u^- - c^-, \quad q_{ct}^-, \quad q_{ds}^-, \quad q_{sb}^-, \quad l_{e\mu}^-, \quad \text{and } l_{\mu\tau}^-. \quad (3.18)$$

² Keep in mind that for example $P_{u_i l_j}^S = P_{u_l}^S$.

³ In the case where one of the flavor numbers is one or zero, there will be no according f_{ij}^- in the evolution basis.

3. The evolution basis

All these distributions evolve independently:

$$\frac{df_{ij}^-}{dt} = P_f^- f_{ij}^-. \quad (3.19)$$

Looking back again at the valence evolution (3.12), one can define the next three basis elements

$$\Sigma_u^- \equiv \sum_i^{n_u} u_i^-, \quad \Sigma_d^- \equiv \sum_i^{n_d} d_i^-, \quad \text{and} \quad \Sigma_l^- \equiv \sum_i^{n_l} l_i^-, \quad (3.20)$$

which introduces minimal mixing in between only these distributions. After some algebra we find

$$\frac{d\Sigma_u^-}{dt} = (P_u^- + n_u \Delta P_{uu}^-) \Sigma_u^- + n_u (\Delta P_{ud}^- \Sigma_d^- + \Delta P_{ul}^- \Sigma_l^-), \quad (3.21)$$

and accordingly for Σ_d^- and Σ_l^- . Up to NLO, it is verified that $P_{ff'} = P_{f\bar{f}'}$, thus $\Delta P_{ff'}^S = 0$ and therefore also this chapter evolves diagonally. This would change when going to NNLO.

Up until now, what we have covered is the so-called non-singlet chapter. If we would we have restricted ourselves to pure QCD, there would be no mixing at all in this region of the evolution basis. The advent of QED introduces coupling between different evolution equations, which can be kept minimal by defining the Σ_f^- distributions, where again $f = u, d, l$. Closely related to them are the so-called singlet distributions

$$\Sigma_f^+ \equiv \sum_i^{n_F} f_i^+, \quad (3.22)$$

where

$$f^+ \equiv f + \bar{f}. \quad (3.23)$$

These distributions evolve as follows:

$$\frac{df^+}{dt} = P_f^+ f^+ + \sum_{f'} \bar{P}_{ff'}^S f'^+ + 2(P_{fg}g + P_{f\gamma}\gamma). \quad (3.24)$$

We can now restrict the mixing of the gluon and photon distributions to as few other ones as possible by defining the singlet distributions as above. Again, after some algebra we find that these are the evolution equations of the second and entangled

3. The evolution basis

sector:

$$\frac{dg}{dt} = P_{gg}g + P_{g\gamma}\gamma + \sum_{f=u,d,l} P_{gf}\Sigma_f^+ \quad (3.25)$$

$$\frac{d\gamma}{dt} = P_{\gamma\gamma}\gamma + P_{\gamma g}g + \sum_{f=u,d,l} P_{\gamma f}\Sigma_f^+ \quad (3.26)$$

$$\frac{d\Sigma_u^+}{dt} = (P_u^+ + n_u\bar{P}_{uu})\Sigma_u^+ + n_u(\bar{P}_{ud}\Sigma_d^+ + \bar{P}_{ul}\Sigma_l^+) + 2n_u(P_{qg}g + P_{u\gamma}\gamma) \quad (3.27)$$

$$\frac{d\Sigma_d^+}{dt} = (P_d^+ + n_d\bar{P}_{dd})\Sigma_d^+ + n_d(\bar{P}_{du}\Sigma_u^+ + \bar{P}_{dl}\Sigma_l^+) + 2n_d(P_{qg}g + P_{d\gamma}\gamma) \quad (3.28)$$

$$\frac{d\Sigma_l^+}{dt} = (P_l^+ + n_l\bar{P}_{ll})\Sigma_l^+ + n_l(\bar{P}_{lu}\Sigma_u^+ + \bar{P}_{ld}\Sigma_d^+) + 2n_l P_{l\gamma}\gamma \quad (3.29)$$

This choice of an evolution basis is not unique. E.g., in [de Florian et al., 2017b] and [de Florian et al., 2017a], sums and differences of Σ_u^+ and Σ_d^u are used. Nevertheless, this does not add any further decoupling but rather increases the size of the evolution equations above.

4. Implementation of QED and QED \otimes QCD splitting kernels

As mentioned in the end of chapter 1, we need to take care of the new arising splitting kernels. Fortunately, these are already calculated, see [de Florian et al., 2017a] and [de Florian et al., 2017b]. Hence, one could implement all these explicit expressions in the according evolution equations, see chapter 3. Nevertheless, this would result in many unnecessary matrix multiplications between kernels and PDFs. The reason for this is that graph topologies do not change when going from pure QCD diagrams to mixed QCD \otimes QED or pure QED ones. To make this explicit, we introduce a new notation by splitting an arbitrary kernel not only into the different orders¹, see (1.5), but also every order into the colour structure, i.e.

$$P_{ij} = \sum_c c P_{ij}^c, \quad (4.1)$$

where the c are prefactors which contain all the well known color structures/ $SU(3)$ group constants, e.g. $c = C_F C_A$. P_{ij}^k will from now on be called color stripped kernels. Their shape can be deduced by looking at the complete kernels, e.g. given in [Ellis and Vogelsang, 1996], chapter 2.5. In the case of pure QCD, this leads to

$$\begin{aligned} \hat{P}_{gg} = & \alpha_s \left(C_A P_{gg}^{C_A} - \frac{4}{3} T_F n_F \delta(1-x) \right) \\ & + \alpha_s^2 \left(C_F T_F \hat{P}_{gg}^{C_F T_F} + C_A T_F P_{gg}^{C_A T_F} + C_A^2 P_{gg}^{C_A^2} \right) \end{aligned} \quad (4.2)$$

$$\begin{aligned} \hat{P}_{gq} = & \alpha_s C_F P_{gq}^{C_F} \\ & + \alpha_s^2 \left(C_F^2 P_{gq}^{C_F^2} + C_F C_A P_{gq}^{C_F C_A} + C_F T_F P_{gq}^{C_F T_F} \right) \end{aligned} \quad (4.3)$$

$$\begin{aligned} \hat{P}_{qg} = & \alpha_s T_F P_{qg}^{T_F} \\ & + \alpha_s^2 \left(C_F T_F P_{qg}^{C_F T_F} + C_A T_F P_{qg}^{C_A T_F} \right) \end{aligned} \quad (4.4)$$

¹ Since just the pure QCD NNLO kernels are completely calculated up to now, here and in the following we restrict ourselves to NLO kernels.

4. Implementation of QED and QED \otimes QCD splitting kernels

$$\begin{aligned}\hat{P}_{qqV} = & \alpha_s C_F P_{qqV}^{C_F} \\ & + \alpha_s^2 \left(C_F^2 P_{qqV}^{C_F^2} + C_A C_F P_{qqV}^{C_A C_F} + C_F T_F P_{qqV}^{C_F T_F} \right)\end{aligned}\quad (4.5)$$

$$\hat{P}_{q\bar{q}V} = \alpha_s^2 \left(C_F^2 - \frac{N_C C_F}{2} \right) P_{q\bar{q}V}^{20} \quad (4.6)$$

$$\hat{P}_{qq'S} = \alpha_s^2 C_F T_F P_{qqS}^{C_F T_F} \quad (4.7)$$

$$\hat{P}_{q\bar{q}'S} = \alpha_s^2 C_F T_F P_{q\bar{q}S}^{C_F T_F} = \alpha_s^2 C_F T_F P_{qqS}^{C_F T_F}, \quad (4.8)$$

where all other kernels, e.g. $\hat{P}_{\gamma l}$, are zero. One can now obtain all kernels involving QED for quarks, leptons, the gluon and the photon² from these expressions. According to the order, (0, 1), (1, 1) or (0, 2), one replaces one or both gluons by a photon, which partly or completely replaces the color by a charge structure. E.g., a loop over every active quark flavor, "coupling" to a gluon, gives rise to a factor $T_F n_F$, where n_F is the number of active flavors. Replacing this by a QED fermion-photon coupling turns this into a loop over all fermions and hence produces a sum over all squared fermionic charges as prefactor instead: $\sum_f N_C^f e_f^2$, where f runs over all lepton and quark flavors. Note that the interaction with a photon is color degenerated³, which add a factor of $N_C^q = N_C = 3$ in the case of quarks and leaves the leptonic case, where $N_C^l = 1$, unchanged. Additionally, in the process called abelization, all diagrams involving three- and four-gluon vertices inheriting from the non-abelian $SU(3)$ gauge invariance of QCD need to be discarded when collecting all diagrams with at least one photon. In the end, one finds that to every abelian QCD diagram of order (1, 0) and (2, 0) there is a unique correspondent of order (0, 1) and (0, 2). In the case of qq -kernels at (1, 1), there are two different ways for every pure QCD diagram leading to the same color-charge structure (see [de Florian et al., 2017a], p. 8 for exemplary diagrams). Section III of [de Florian et al., 2017a] gives a more detailed overview over this procedure. The kernels (reduced by the pure QCD contributions given above) are

$$\tilde{P}_{gg} = \alpha_e \alpha_s T_F \sum_q e_q^2 \delta(1-x) \quad (4.9)$$

$$\tilde{P}_{gq} = \alpha_e \alpha_s C_F e_q^2 P_{gq}^{C_F^2} \quad (4.10)$$

$$\tilde{P}_{qq} = \alpha_e \alpha_s e_q^2 T_F P_{qq}^{C_F T_F} \quad (4.11)$$

$$\begin{aligned}\tilde{P}_{qqV} = & \alpha_e e_q^2 P_{qqV}^{C_F} + \alpha_e^2 \left(e_q^4 P_{qqV}^{C_F^2} + e_q^2 \sum_f N_C^f e_f^2 P_{qqV}^{C_F T_F} \right) \\ & + \alpha_e \alpha_s 2e_q^2 C_F P_{qqV}^{C_F^2}\end{aligned}\quad (4.12)$$

² Pure QCD kernels for leptons and photons are of course zero.

³ It is for this reason that one also has to average over the color of incoming particles in the case of diagrams which include QED.

4. Implementation of QED and QED \otimes QCD splitting kernels

$$\tilde{P}_{q\bar{q}V} = \alpha_e^2 e_q^4 P_{q\bar{q}V}^{20} + \alpha_e \alpha_s 2e_q^2 C_F P_{q\bar{q}V}^{20} \quad (4.13)$$

$$\tilde{P}_{qq'S} = \alpha_e^2 N_C e_q^2 e_{q'}^2 P_{qq'S}^{CF T_F} \quad (4.14)$$

$$\tilde{P}_{q\bar{q}'S} = \tilde{P}_{qq'S} \quad (4.15)$$

$$\begin{aligned} \tilde{P}_{\gamma\gamma} = & -\alpha_e \frac{2}{3} \sum_f N_C^f e_f^2 \delta(1-x) + \alpha_e^2 \sum_f N_C^f e_f^4 P_{gg}^{CF T_F} \\ & - \alpha_e \alpha_s \sum_q e_q^2 \delta(1-x) \end{aligned} \quad (4.16)$$

$$\begin{aligned} \tilde{P}_{\gamma f} = & \alpha_e e_f^2 P_{gq}^{CF} + \alpha_e^2 \left(e_f^4 P_{gq}^{CF^2} + e_f^2 \sum_f N_C^f e_f^2 P_{gq}^{CF T_F} \right) \\ & \left[+ \alpha_e \alpha_s e_f^2 C_F P_{gq}^{CF^2} \right] \end{aligned} \quad (4.17)$$

$$\begin{aligned} \tilde{P}_{f\gamma} = & \alpha_e e_f^2 P_{qg}^{T_F} + \alpha_e^2 e_f^4 N_C^f P_{qg}^{CF T_F} \\ & \left[+ \alpha_e \alpha_s N_C C_F e_f^2 P_{qg}^{CF T_F} \right] \end{aligned} \quad (4.18)$$

$$\tilde{P}_{llV} = \alpha_e e_l^2 P_{qqV}^{CF} + \alpha_e^2 \left(e_l^4 P_{qqV}^{CF^2} + e_l^2 \sum_f N_C^f e_f^2 P_{qqV}^{CF T_F} \right) \quad (4.19)$$

$$\tilde{P}_{l\bar{l}V} = \alpha_e^2 e_l^4 P_{q\bar{q}V}^{20} \quad (4.20)$$

$$\tilde{P}_{ff'S} = \alpha_e^2 N_C^{f'} e_{f'}^2 P_{qqS}^{CF T_F} \quad (4.21)$$

$$\tilde{P}_{f\bar{f}'} = \tilde{P}_{ff'} \quad (4.22)$$

where the terms in the square brackets only need be taken into account when the fermion f is a quark. For the last two kernels, at least one of the fermions f or f' has to be a lepton. Furthermore, the complete kernels P up to NLO can be obtained by adding \hat{P} and \tilde{P} .

All this work now bears fruits when one implements the complete kernels in `chilipdf`. It now becomes rather obvious, where one can factorize kernels or PDFs to save runtime. Another possibility is to precalculate convolutions. The general rule goes as follows: Let n be the number, a specific kernel gets convoluted with and m the number of equations, this kernel appears in. If $n > m$, factorize this kernel in every equation. If otherwise, precalculate the convolution with every PDF. If $n = m$, both procedures save the same amount of evaluations. We now give every full LO evolution equation in terms of color-stripped kernels. If one should precalculate a certain convolution, this is indicated with square brackets, i.e. $[P_{ab}]$.

$$\frac{dg^{\text{LO}}}{dt} = \alpha_s \left(C_F P_{gq}^{CF} \left(\Sigma_u^+ + \Sigma_d^+ \right) + C_A P_{gg}^{CA} g - \frac{4}{3} T_F n_F \delta(1-x) g \right) \quad (4.23)$$

$$\frac{d\gamma^{\text{LO}}}{dt} = \alpha_e \left(P_{gq}^{CF} \left(e_u^2 \Sigma_u^+ + e_d^2 \Sigma_d^+ + e_l^2 \Sigma_l^+ \right) - \frac{4}{3} \sum_f N_C^f e_f^2 \delta(1-x) \gamma \right) \quad (4.24)$$

4. Implementation of QED and QED \otimes QCD splitting kernels

$$\begin{aligned} \frac{d\Sigma_q^{+\text{LO}}}{dt} = & \left(\alpha_s C_F + \alpha_e e_q^2 \right) P_{qq}^{C_F} \Sigma_q^+ \\ & + 2n_q \left(\alpha_s T_F [P_{qg}^{T_F} g] + \alpha_e N_C e_q^2 [P_{qg}^{T_F} \gamma] \right), \end{aligned} \quad (4.25)$$

where $q = u, d$

$$\frac{d\Sigma_l^{+\text{LO}}}{dt} = \alpha_e \left(e_l^2 P_{qqV}^{C_F} \Sigma_l^+ + 2n_l e_l^2 [P_{qg}^{T_F} \gamma] \right) \quad (4.26)$$

$$\frac{d\left(\Sigma_q^-, q_{ij}^\pm\right)^{\text{LO}}}{dt} = \left(\alpha_s C_F + \alpha_e e_q^2 \right) P_{qqV}^{C_F} \left(\Sigma_q^-, q_{ij}^\pm \right), \quad (4.27)$$

where $q = u, d$ and i, j are flavors

$$\frac{d\left(\Sigma_l^-, l_{ij}^\pm\right)^{\text{LO}}}{dt} = \alpha_e e_l^2 P_{qqV}^{C_F} \left(\Sigma_l^-, l_{ij}^\pm \right), \quad (4.28)$$

where i, j are leptonic flavors

The virtual corrections proportional to $\delta(1-x)$ in the equations for g and γ become unity matrices when going from kernels to matrices. As can be seen above, precalculations are only favorable in the case of $P_{qg}^{T_F}$. This is quite similar to the case of NLO, which equations are given in appendix B.

5. Numerical Results

We are testing the implementation with a toy model set of PDFs, which aims to describe the proton, at the starting scale $\mu = \sqrt{2}\text{GeV}$ from [The QCD/SM Working Group, 2002] for quarks and gluons. Due to a lack of experimental data, leptons and the photon are set to zero at this scale.

A reliable check for the implementation are the sum rules. Since PDFs are normalized with respect to the according number of partons in the proton, the integral over the whole x range of the difference between one specific flavor and antiflavor needs to reproduce the according number of valence particles in the proton at all scales μ . Thus, a numerical comparison of

$$\int_0^1 dx u^-(x) - 2 = 0 \quad (5.1)$$

$$\text{and } \int_0^1 dx d^-(x) - 1 = 0 \quad (5.2)$$

at starting and target scale μ_0 and μ provides a good check.

Furthermore, one can make use of the fact that the expectation value of the momentum fraction of the proton itself needs to be 1. Momentum conservation implies that again this needs to be true at all energies. To get the PDF of the proton, we just add up all constituents, hence the momentum sum rule reads

$$\int_0^1 dx x \left(g(x) + \gamma(x) + \sum_{f=u,d,l} \Sigma_f^+ \right) - 1 = 0. \quad (5.3)$$

This check is of even greater importance since it directly includes the new photon and lepton PDFs.

However, one expects deviations from these results after the evolution for one reasons: Due two self-interactions the gluon PDF becomes steeper at high energies. Since the numerical approximation of the integrals in the sum rules cannot start at exactly zero¹, one ignores an increasing contribution to the integral for growing μ . To demonstrate this effect, let us start the integration at $x = 10^{-8}$ and then introduce a new subgrid ranging from $x = 10^{-11}$ to $x = 10^{-8}$ with 23 subpoints. In the first case, for a pure gluon evolution at LO we fulfill the momentum sum rule with a difference of order 10^{-5} , in the second one we improve to 10^{-7} . In the following numerical

¹ The reason for this is that `chilipdf` actually works on a grid on $\log(x)$, not x itself.

5. Numerical Results

calculations we on subgrids between the values $x = 10^{-11}, 10^{-8}, 10^{-4}, 0.5, 1$, where the subgrids have (23, 23, 31, 23) gridpoints.

Nevertheless, one can compare this deviations with the one occuring in the case of pure QCD. If both are of the same order of magnitude, this is a huge hint for properly implemented evolution equations. Table 5.1 shows the numerically evaluated sum rules at LO and NLO. As it can be seen, all sum rules are correctly reproduced after the QCD \otimes QED evolution. Another positive check was the successful reproduction of PDFs, which were evolved by the pure QCD-evolver, at LO and NLO.

Of particular interest is table 5.2, where the different runtimes of the pure QCD and QCD \otimes QED evolvers get compared. We see, that the runtime of the QED-enhanced evolution just increases by a factor of 3 to 4, which is much less than the factor of a naive ansatz: If one would choose a brute-force ansatz and just evaluates the 5×5 instead of the 2×2 , just in the singlet sector at LO alone the runtime would increase by a factor of $\frac{25}{4} \approx 6$.

Summing up all the numerical results, this project can be considered a success. The new kernels, arising from the QED interactions, were implemented properly and the additional runtime could be significantly reduced through the usage of color stripped kernels.

Table 5.1.: Comparing differences of sum rules at starting and target scale for pure QCD and QCD \otimes QED evolution at LO and NLO. The flavor numbers are $n_u = 2$ and $n_d = n_l = 3$ and the parametrizations at μ_0 are described at the beginning of this chapter. At the starting scale, the sum rules take the values $2 - \int u^- = 1.012 \cdot 10^{-8}$, $1 - \int d^- = 6.071 \cdot 10^{-9}$ and $1 - \int x(g + \gamma + \Sigma_u^+ + \Sigma_d^+ + \Sigma_l^+) = 2.234 \cdot 10^{-8}$.

sum rule, order	difference between sum rule at μ_0 and μ , pure QCD	difference between sum rule at μ_0 and μ , QCD \otimes QED
u^- , LO	$-3.891 \cdot 10^{-8}$	$-3.995 \cdot 10^{-7}$
d^- , LO	$-2.328 \cdot 10^{-8}$	$-2.343 \cdot 10^{-8}$
momentum, LO	$2.032 \cdot 10^{-7}$	$2.033 \cdot 10^{-7}$
u^- , NLO	$-1.645 \cdot 10^{-7}$	$-1.621 \cdot 10^{-7}$
d^- , NLO	$-9.731 \cdot 10^{-8}$	$-9.696 \cdot 10^{-8}$
momentum, NLO	$2.223 \cdot 10^{-7}$	$2.225 \cdot 10^{-8}$

5. Numerical Results

Table 5.2.: Comparing runtimes of an evolver optimized for pure QCD evolution with the new one optimized for QCD \otimes QED evolution (for $n_l = 0$ and $n_l = 3$) with the approach of color stripped matrices. The runtime is an average over 100 evolutions computed with a notebook version of an AMD Ryzen 5 processor.

order	pure QCD evolver, in ms	QCD \otimes QED evolver, in ms, $n_l = 3$	relative factor	QCD \otimes QED evolver, in ms, $n_l = 0$	relative factor
LO	$4.747 \cdot 10^1$	$1.602 \cdot 10^2$	3.375	$1.247 \cdot 10^2$	2.627
NLO	$1.072 \cdot 10^2$	$4.151 \cdot 10^2$	3.872	$3.675 \cdot 10^2$	3.428

A. Explicit shape of coupled RGE solutions

In the following we will give all right-hand-sides of the NLO and NNLO solutions of $r_e(r_s)$ and $\delta_r(r_s)$ of chapter 2. The NLO solutions contain coefficients A_{\dots} and B_{\dots} , which implicitly depend on the expansion parameters ϵ_s and ϵ_e .

$$A_{0e} = 1 + \epsilon_e b_{10}^e \alpha_e^0 + \epsilon_s b_{01}^e \alpha_e^0 \quad (\text{A.1})$$

$$A_{1e} = 1 + b_0^e \frac{\alpha_e^0}{\alpha_s^0} + \epsilon_e b_{10}^e \alpha_e^0 + \epsilon_s b_{01}^e b_0^e \alpha_e^0 \quad (\text{A.2})$$

$$A_{2e} = b_0^e \frac{\alpha_e^0}{\alpha_s^0} \quad (\text{A.3})$$

$$B_{0e} = 1 + \epsilon_s b_{10}^s \alpha_s^0 \quad (\text{A.4})$$

$$B_{1e} = 1 + b_0^e \frac{\alpha_e^0}{\alpha_s^0} + \epsilon_s b_{10}^s \alpha_e^0 \quad (\text{A.5})$$

$$A_{0\delta} = 1 + \epsilon_e b_{01}^s \alpha_e^0 + \epsilon_s b_{10}^s b_0^e \alpha_e^0 \quad (\text{A.6})$$

$$A_{1\delta} = 1 + b_0^e \frac{\alpha_e^0}{\alpha_s^0} + \epsilon_e b_{01}^s \alpha_e^0 + \epsilon_s b_{10}^s b_0^e \alpha_e^0 \quad (\text{A.7})$$

$$A_{2\delta} = b_0^e \frac{\alpha_e^0}{\alpha_s^0} \quad (\text{A.8})$$

$$B_{0\delta} = 1 + \epsilon_s b_{10}^s \alpha_s^0 \quad (\text{A.9})$$

$$B_{1\delta} = 1 + b_0^e \frac{\alpha_e^0}{\alpha_s^0} + \epsilon_s b_{10}^s b_0^e \alpha_e^0 \quad (\text{A.10})$$

The fully written out results are

$$F_e^{\text{NLO}}(r_s) = r_s - \frac{2A_{2e}A_{0e} - 2A_{2e}B_{0e} - A_{1e}B_{1e} + B_{1e}^2}{A_{2e}\sqrt{B_{1e}^2 - 4A_{2e}B_{0e}}} \cdot \text{artanh}\left(\frac{2A_{2e}r_s + B_{1e}}{\sqrt{B_{1e}^2 - 4A_{2e}B_{0e}}}\right) + \frac{A_{1e} - B_{1e}}{2A_{2e}} \cdot \ln(A_{2e}r_s^2 + B_{1e}r_s + B_{0e}) \quad (\text{A.11})$$

$$F_\delta^{\text{NLO}}(r_s) = \frac{2A_{2\delta}A_{0\delta} - 2A_{2\delta}B_{0\delta} - A_{1\delta}B_{1\delta} + B_{1\delta}^2}{A_{2\delta}\sqrt{B_{1\delta}^2 - 4A_{2\delta}B_{0\delta}}} \cdot \text{artanh}\left(\frac{2A_{2\delta}r_s + B_{1\delta}}{\sqrt{B_{1\delta}^2 - 4A_{2\delta}B_{0\delta}}}\right) + \frac{A_{1\delta} - B_{1\delta}}{2A_{2\delta}} \cdot \ln(A_{2\delta}r_s^2 + B_{1\delta}r_s + B_{0\delta}) \quad (\text{A.12})$$

A. Explicit shape of coupled RGE solutions

The areatangens hyperbolicus functions in the formulae above are the defined for the absolute value of their argument being smaller than 1. E.g. for F_e^{NLO} , this means that r_s ranges approximately from -1 to 5.5 . This corresponds (using the numerical solution of the inversion of (2.15)) to energies between 0 GeV to approximately 10^{18} GeV , which is the same order of magnitude as the Landau pole of QED.

$$\begin{aligned}
F_e^{\text{NNLO}}(r_s) = & r_s + (\alpha_s^0)^2 \left(\epsilon_s^2 \frac{b_{20}^s - b_{02}^e + b_{10}^s(b_{01}^e - b_{10}^s)}{1 + r_s} - \epsilon_e \alpha_e^0 \frac{\epsilon_e b_{20}^e + \epsilon_s b_0^e b_{10}^e(b_{10}^s - b_{01}^e)}{b_0^e(\alpha_s^0 + \alpha_e^0 b_0^e r_s)} \right) \\
& - \epsilon_e \alpha_s^0 \frac{1}{b_0^e(1 + r_s)(\alpha_s^0 + \alpha_e^0 b_0^e r_s)} \cdot \left\{ \epsilon_s \alpha_s^0 b_{01}^e b_{01}^s \right. \\
& \quad - \alpha_e^0 \alpha_s^0 b_{10}^e [\epsilon_e b_{10}^e + \epsilon_s b_0^e(b_{10}^s - b_{01}^e)] \\
& \quad \left. + \alpha_e^0 [\alpha_s^0 b_{10}^e(\epsilon_e b_{10}^e + \epsilon_s b_0^e(b_{10}^s - b_{01}^e)) - \epsilon_s b_{01}^e b_{01}^s b_0^e] r_s \right\} \\
& \times \text{artanh} \left(\frac{\alpha_s^0 + \alpha_e^0 b_0^e}{\alpha_s^0 - \alpha_e^0 b_0^e} \right) \\
& + \epsilon_e \alpha_e^0 \frac{1}{b_0^e(1 + r_s)(\alpha_s^0 + \alpha_e^0 b_0^e r_s)} \cdot \left\{ \epsilon_s \alpha_s^0 b_{10}^e b_{01}^s \right. \\
& \quad \left. - \alpha_e^0 [\epsilon_e (b_{10}^e)^2 (1 + r_s) - \epsilon_s b_{10}^e b_{01}^s r_s - \epsilon_s b_0^e b_{10}^e (b_{01}^e - b_{10}^s)(1 + r_s)] \right\} \\
& \times \text{artanh} \left(\frac{\alpha_s^0 + \alpha_e^0 b_0^e + 2\alpha_e^0 b_0^e r_s}{\alpha_s^0 - \alpha_e^0 b_0^e} \right) \\
& + \frac{\alpha_s^0}{2b_0^e} \left\{ -\frac{2}{\alpha_s^0 - \alpha_e^0 b_0^e} \cdot \left[\epsilon_e^2 \alpha_e^0 \alpha_s^0 (b_0^e)^2 + \epsilon_s b_0^e ((\alpha_e^0 b_0^e - \alpha_s^0)(b_{01}^e - b_{10}^s) \right. \right. \\
& \quad \left. \left. + \epsilon_e \alpha_e^0 \alpha_s^0 (b_{01}^e b_{01}^s + b_{10}^e b_{10}^s - b_{11}^e)) \right] \ln(1 + r_s) \right. \\
& \quad + \frac{2\epsilon_e}{\alpha_s^0 - \alpha_e^0 b_0^e} \cdot \left[b_{10}^e (\alpha_s^0 - \alpha_e^0 b_0^e + \epsilon_s \alpha_e^0 \alpha_s^0 b_{10}^e) \right. \\
& \quad \left. + \epsilon_s \alpha_e^0 \alpha_s^0 b_0^e (b_{01}^e b_{01}^s + b_{10}^e b_{10}^s - b_{11}^e) \right] \ln(\alpha_s^0 + \alpha_e^0 b_0^e r_s) \\
& \quad + \frac{\alpha_s^0 \epsilon_e}{(1 + r_s)(\alpha_s^0 + \alpha_e^0 b_0^e r_s)} \cdot \left[\epsilon_s \alpha_s^0 b_{01}^e b_{01}^s + \alpha_e^0 b_{10}^e (\epsilon_e b_{10}^e + \epsilon_s b_0^e (b_{10}^s - b_{10}^s)) \right. \\
& \quad \left. + \alpha_e^0 (\epsilon_e (b_{10}^e)^2 + \epsilon_s b_0^e (b_{01}^e (b_{01}^s - b_{10}^s))) r_s \right] \\
& \quad \left. \times \ln \left(\frac{(1 + r_s)(\alpha_s^0 + \alpha_e^0 b_0^e r_s)}{\alpha_s^0} \right) \right\} \tag{A.13}
\end{aligned}$$

A. Explicit shape of coupled RGE solutions

$$\begin{aligned}
F_{\delta}^{\text{NNLO}}(r_s) = \alpha_s^0 \epsilon_e \Bigg\{ & \epsilon_e \frac{\alpha_e^0 \alpha_s^0}{b_0^e (\alpha_s^0 + \alpha_e^0 b_0^e r_s)} \cdot (b_{01}^s b_{10}^s - b_{02}^s) \\
& - \frac{\alpha_s^0 b_{01}^s \left[\epsilon_e \alpha_s^0 b_{10}^s + \alpha_e^0 \left(\epsilon_e b_{10}^e (1 + r_s) + \epsilon_e b_0^e (b_{10}^s + 2b_{10}^s r_s - b_{01}^e (1 + r_s)) \right) \right]}{b_0^e (1 + r_s) (\alpha_s^0 + \alpha_e^0 b_0^e r_s)} \\
& \times \left[\text{artanh} \left(\frac{\alpha_s^0 + \alpha_e^0 b_0^e}{\alpha_s^0 - \alpha_e^0 b_0^e} \right) + \text{artanh} \left(\frac{\alpha_s^0 + \alpha_e^0 b_0^e + 2\alpha_e^0 b_0^e r_s}{\alpha_s^0 - \alpha_e^0 b_0^e} \right) \right] \\
& - \epsilon_s \frac{\alpha_e^0 \alpha_s^0 (b_{01}^e b_{01}^s + b_{01}^s b_{10}^s - b_{11}^s)}{\alpha_s^0 - \alpha_e^0 b_0^e} \ln(1 + r_s) \\
& + \left[\frac{b_{01}^s}{b_0^e} + \epsilon_s \alpha_e^0 \alpha_s^0 \frac{b_{01}^e b_{01}^s - b_{01}^s b_{10}^s + b_{11}^s}{\alpha_s^0 - \alpha_e^0 b_0^e} \right] \ln(\alpha_s^0 + \alpha_e^0 b_0^e r_s) \\
& + \frac{\alpha_s^0 b_{01}^s \left[\epsilon_s \alpha_s^0 b_{10}^s + \alpha_e^0 \left(\epsilon_e b_{10}^e (1 + r_s) + \epsilon_s b_0^e (b_{01}^e - b_{10}^s + b_{01}^e r_s) \right) \right]}{2b_0^e (1 + r_s) (\alpha_s^0 + \alpha_e^0 b_0^e r_s)} \\
& \times \ln \left(\frac{(1 + r_s) (\alpha_s^0 + \alpha_e^0 b_0^e r_s)}{\alpha_s^0} \right) \Bigg\} \tag{A.14}
\end{aligned}$$

Note that there are no leading r_s terms in the F_{δ} -functions, which can be traced back to the vanishing LO solution of δ_r . It is also evident that in δ_r all corrections are at least of order ϵ_e . One could have expected that due to the cancellations of all pure QCD terms in (2.20) via the -1 at the end.

B. Full NLO color-stripped evolution equations

Applying the techniques discussed at the end of chapter 4, we arrive at

$$\begin{aligned} \frac{dg^{\text{NLO}}}{dt} = & \alpha_s^2 \left((C_F C_A P_{gq}^{C_F C_A} + C_F T_F n_F P_{gq}^{C_F T_F} + C_F^2 P_{gq}^{C_F^2}) (\Sigma_u^+ + \Sigma_d^+) \right. \\ & \left. + (C_F T_F n_F P_{gg}^{C_F T_F} + C_A T_F n_F P_{gg}^{C_A T_F} + C_A^2 P_{gg}^{C_A^2}) g \right) \\ & + \alpha_s \alpha_e \left(C_F P_{gq}^{C_F^2} (e_u^2 \Sigma_u^+ + e_d^2 \Sigma_d^+) \right. \\ & \left. + C_F N_C \sum_q e_q^2 P_{gg}^{C_F T_F} \gamma + 4 C_F N_C \sum_q e_q^2 \delta(1-x) \gamma \right. \end{aligned} \quad (\text{B.1})$$

$$\left. - 4 T_F \sum_q e_q^2 \delta(1-x) g \right) \quad (\text{B.2})$$

$$\begin{aligned} \frac{d\gamma^{\text{NLO}}}{dt} = & \alpha_e^2 \sum_f N_C^f e_f^2 P_{gq}^{C_F T_F} (e_u^2 \Sigma_u^+ + e_d^2 \Sigma_d^+ + e_l^2 \Sigma_l^+) \\ & + P_{gq}^{C_F^2} \left((\alpha_e^2 e_u^4 + \alpha_s \alpha_e C_F e_u^2) \Sigma_u^+ + (\alpha_e^2 e_d^4 + \alpha_s \alpha_e C_F e_d^2) \Sigma_d^+ + \alpha_e^2 e_l^4 \Sigma_l^+ \right) \\ & + P_{gg}^{C_F T_F} \left(\alpha_s \alpha_e T_F \sum_q e_q^2 g + \alpha_e^2 \sum_f N_C^f e_f^4 \gamma \right) \\ & + \alpha_s \alpha_e 4 \sum_q e_q^2 (T_F \delta(1-x) g \\ & \quad - C_F N_C \delta(1-x) \gamma) \end{aligned} \quad (\text{B.3})$$

B. Full NLO color-stripped evolution equations

$$\begin{aligned}
\frac{d\Sigma_q^{+\text{NLO}}}{dt} = & 2n_q \left((\alpha_s^2 C_F T_F + \alpha_s \alpha_e T_F e_q^2) [P_{qg}^{C_F T_F} g] + \alpha_s^2 C_A T_F [P_{gq}^{C_A T_F} g] \right) \\
& + 2n_q N_C (\alpha_e^2 e_q^4 + \alpha_s \alpha_e C_F e_q^2) [P_{qg}^{C_F T_F} \gamma] \\
& + 2n_q P_{qqS}^{C_F T_F} \left(\alpha_e^2 N_C e_q^2 e_l^2 \Sigma_l^+ \right. \\
& \quad \left. + (\alpha_s^2 C_F T_F + \alpha_e^2 e_q^2 N_C e_{q'}^2) \Sigma_{q'}^+ \right), \\
& + \alpha_s^2 \left(C_F^2 P_{qqV}^{C_F^2} + C_F T_F n_F P_{qqV}^{C_F T_F} + C_F C_A P_{qqV}^{C_F C_A} \right. \\
& \quad \left. + \left(C_F^2 - \frac{N_C C_F}{2} \right) P_{q\bar{q}V}^{C_F^2} + 2n_q C_F T_F P_{qqS}^{C_F T_F} \right) \Sigma_q^+ \\
& + \alpha_s \alpha_e 2e_q^2 C_F (P_{qqV}^{C_F^2} + P_{q\bar{q}}^{C_F^2}) \Sigma_q^+ \\
& + \alpha_e^2 \left(e_q^4 (P_{qqV}^{C_F^2} + P_{q\bar{q}V}^{C_F^2} + 2n_q N_C P_{qqS}^{C_F T_F}) \right. \\
& \quad \left. + e_q^2 \sum_f N_C^f e_f^2 P_{qqV}^{C_F T_F} \right) \Sigma_q^+
\end{aligned} \tag{B.4}$$

where $q = u, d$ and $q' = d, u$

$$\begin{aligned}
\frac{d\Sigma_l^{+\text{NLO}}}{dt} = & \alpha_e^2 \left(2n_l e_l^4 [P_{qg}^{C_F T_F} \gamma] \right. \\
& + 2n_l e_l^2 P_{qqS}^{C_F T_F} (e_u^2 \Sigma_u^+ + e_d^2 \Sigma_d^+) \\
& + (e_l^4 (P_{qqV}^{C_F^2} + P_{q\bar{q}V}^{C_F^2} + 2n_l P_{qqS}^{C_F T_F}) \\
& \quad \left. + e_l^2 \sum_f N_C^f e_f^2 P_{qqV}^{C_F T_F}) \Sigma_l^+ \right)
\end{aligned} \tag{B.5}$$

$$\begin{aligned}
\frac{d(\Sigma_q^-, q_{ij}^-)^{\text{NLO}}}{dt} = & \left\{ \alpha_s^2 \left(C_F^2 P_{qqV}^{C_F^2} + C_F T_F n_F P_{qqV}^{C_F T_F} + C_F C_A P_{qqV}^{C_F C_A} - \left(C_F^2 - \frac{N_C C_F}{2} \right) P_{q\bar{q}V}^{C_F^2} \right) \right. \\
& + \alpha_s \alpha_e 2C_F e_q^2 (P_{qqV}^{C_F^2} - P_{q\bar{q}V}^{C_F^2}) \\
& \left. + \alpha_e^2 \left(e_q^4 (P_{qqV}^{C_F^2} - P_{q\bar{q}V}^{C_F^2}) + e_q^2 \sum_f N_C^f e_f^2 P_{qqV}^{C_F T_F} \right) \right\} (\Sigma_q^-, q_{ij}^-)
\end{aligned} \tag{B.6}$$

where $q = u, d$ and i, j are flavors

B. Full NLO color-stripped evolution equations

$$\frac{d(\Sigma_l^-, l_{ij}^-)^{\text{NLO}}}{dt} = \alpha_e^2 (e_l^4 (P_{qqV}^{C_F^2} - P_{q\bar{q}V}^{C_F^2}) + e_l^2 \sum_f N_C^f e_f^2 P_{qqV}^{C_F T_F}) (\Sigma_l^-, l_{ij}^-) \quad (\text{B.7})$$

where i, j are leptonic flavors

$$\begin{aligned} \frac{dq_{ij}^{+\text{NLO}}}{dt} = & \left\{ \alpha_s^2 \left(C_F^2 P_{qqV}^{C_F^2} + C_F T_F n_F P_{qqV}^{C_F T_F} + C_F C_A P_{qqV}^{C_F C_A} \right. \right. \\ & + \left. \left(C_F^2 - \frac{N_C C_F}{2} \right) P_{q\bar{q}V}^{C_F^2} \right) \\ & + \alpha_s \alpha_e 2 C_F e_q^2 (P_{qqV}^{C_F^2} + P_{q\bar{q}V}^{C_F^2}) \\ & + \alpha_e^2 \left(e_q^4 (P_{qqV}^{C_F^2} + P_{q\bar{q}V}^{C_F^2}) + e_q^2 \sum_f N_C^f e_f^2 P_{qqV}^{C_F T_F} \right) \Big\} q_{ij}^+ \quad (\text{B.8}) \end{aligned}$$

where $q = u, d$ and i, j are flavors

$$\frac{dl_{ij}^{+\text{NLO}}}{dt} = \alpha_e^2 \left(e_l^4 (P_{qqV}^{C_F^2} + P_{q\bar{q}V}^{C_F^2}) + e_l^2 \sum_f N_C^f e_f^2 P_{qqV}^{C_F T_F} \right) l_{ij}^+ \quad (\text{B.9})$$

where i, j are leptonic flavors

Again, convolutions in square brackets are evaluated first. Additionally to the procedure at LO, all sums of kernels are precalculated to minimize matrix multiplications. The added contributions proportional to $\delta(1-x)$ in the g and γ evolution equations are there to cancel the virtual parts of $P_{gg}^{C_F T_F}$. The reason for this is that there cannot be a virtual diagram (a diagram without radiation of particles) of a gluon/photon splitting into a photon/gluon due to conservation of color.

Bibliography

- [Bertone et al., 2015] Bertone, V., Carrazza, S., Pagani, D., and Zaro, M. (2015). On the Impact of Lepton PDFs. *arXiv:hep-ph/1508.07002v2*.
- [Billis et al., 2019] Billis, G., Tackmann, F. J., and Talbert, J. (2019). Higher-Order Sudakov Resummation in Coupled Gauge Theories. *arXiv:hep-ph/1907.02971*.
- [de Florian et al., 2017a] de Florian, D., Sborlini, G. F. R., and Rodrigo, G. (2017a). QED corrections to the Altarelli-Parisi splitting functions. *Eur. Phys. J. C* **76** (2016) no.5, 282, *arXiv:hep-ph/1512.00612v3*.
- [de Florian et al., 2017b] de Florian, D., Sborlini, G. F. R., and Rodrigo, G. (2017b). Two-loop QED corrections to the Altarelli-Parisi splitting functions. *JHEP* **10** (2016) 056, *arXiv:hep-ph/1606.02887v3*.
- [Ellis and Vogelsang, 1996] Ellis, R. K. and Vogelsang, W. (1996). The evolution of parton densities beyond leading order. *arXiv:hep-ph/9602356v1*.
- [Peskin and Schroeder, 1995] Peskin, M. E. and Schroeder, D. V. (1995). *An Introduction of Quantum Field Theory*. Westview Press, Colorado.
- [Roth and Weinzierl, 2004] Roth, M. and Weinzierl, S. (2004). QED corrections to the evolution of parton distributions. *Phys.Lett.B* **590**:190-198,2004, *arXiv:hep-ph/0403200v1*.
- [The QCD/SM Working Group, 2002] The QCD/SM Working Group (2002). Report of the Working Group on Quantum ChromoDynamics and the Standard Model for the Workshop “JPhysics at TeV Colliders”. *arXiv:hep-ph/0204316v1*.